

Optoelectronic transitions in Gold spherical Nanoparticles: A Simulation Study

Amit Kumar*

Abstract

There has been intense interest in metallic gold nanoparticles as drug-delivery agent and sensors due to recent applications in biomedical field. For the successful development of biomedical sensors based on metallic nanoparticles, electro-optic interactions have to be studied. This study examined extinction spectra, electric field intensity, and their variations due to various semiconductor medium, for gold nanoparticles, using Nanosphere Optics Lab Field Simulator which is based on Mie's theory of scattering by sphere. The peak extinction wavelength and bandwidth are found to get varied with size of the gold nanoparticle, in four different regimes. Asymmetric distributions of electric fields are observed in particles typically larger than 25nm. The significant differences are found in the results due to changes in the embedding medium. The gold nanoparticles' unique tunable electro-optical properties may therefore be useful for medical, health care, industrial catalysts, and other consumer products. The study shows improved results may be obtained in the medium size range *i.e.* 25-75nm. In addition, the selectivity can be improved linearly as the refractive index of the host material increases.

Keywords: Au nanoparticles, electric field variations, extinction coefficient, embedded medium dependences.

* Department of Electronics, Bhaskaracharya College of Applied Sciences, University of Delhi, South West Delhi, New Delhi, 110075, India; amit.kumar@bcas.du.ac.in

1. Introduction

Nanoparticles can be applied in many ways in the real world applications, making them valuable to the next generation technologies. Semiconductor nanoparticles, used mostly in optoelectronics applications, are among the most studied of these materials. The technological advancement and knowledge have made easier fabrication of metallic nanoparticles too [1]. However, metallic nanoparticles have received less exploration than their semiconductor counterparts. In recent years, there has been a steadily growing interest in using these nanoparticles for biomedical applications, including drugs delivery, hyperthermia, photoablation therapy, imaging, and biosensors [2]. Since decades, metallic nanoparticles have fascinated scientists working in the fields of biomedical sciences and engineering. Gold has been thought of as having an immortal nature (*e.g.* resistance to chemical corrosion) and associated with longevity, so it has been used as a medicine to promote longevity [3]. Indian medicine, *ayurveda*, has been around for thousands of years and involves various herbs, metals and minerals being used as medicine. The gold ash (*Swarna Bhasma*), a traditional component of Indian *ayurvedic* medicine, is characterized by globular gold particles (56-57 nm) [4]. *Swarna bhasma* which is usually taken by mouth with honey, ghee, or milk to treat several clinical conditions [5, 6]. The potential application of this technology in drug delivery and noninvasive imaging offers several advantages over conventional pharmaceuticals [7]. In liver function tests and histological investigations of albino mice, acute oral administration (continuous for 8 weeks; 10 mg/20g b.w./day) of *Swarna bhasma* showed no toxic effects [8]. There is a possibility that some *Swarna bhasma* particles get absorbed directly into the blood stream through the sublingual route. In order to be effective, nanoparticles must be stable, biocompatible, and selectively directed to certain sites after their systematic administration. For example, by using a more precise identification technique, one can target cancer cells. This can be done by coating the nanoparticles with a ligand that binds specifically to the target cells. The nanoparticles can also serve as a platform for attaching numerous therapeutic materials, which will increase their concentration at the pathological site. The small

particle size combined with a stealth ligand on the surface of the particles allows them to hide from the body's immune system, allowing them to circulate in the blood for a longer period of time. Recent years have seen an increase in the application of nanoparticles, such as magnetic nanoparticles (iron oxide), gold and silver nanoparticles, and nanoshells and nanocages, as therapeutic agents [9]. Nanoparticles made of gold (Au) have various important applications, such as nano-biotechnology, biosensor technology, visualization of cell structures, targeted drug delivery, and water purification [10]. The optoelectronic transitions play an important role in making recent Au-nanoparticles based biomedical sensors. This paper present a simulation study on how gold nanoparticles behave when in contact with light, based on the Nanosphere Optics Lab Field Simulator [11], in addition to similar work by many groups in recent years [12-14]. The model is based on Mie's theory of electromagnetic radiation scattering by homogeneous spheres. In this work, we investigated the variations in electric field intensity and extinction spectra of Au-spherical nanoparticle with the variations in size, light polarization, and semiconducting medium, in continuation with the previous similar work done on silver nanoparticle [14].

2. Theoretical discussion

The underlying physics of metallic nanoparticles differs significantly from the physics of semiconductor quantum dots. The conduction band electron cloud in small spherical metallic nanoparticles exposed to light oscillates coherently, because of the oscillating electric field, as shown in the schematic diagram in Fig. 1.

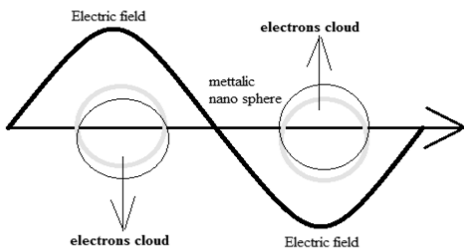


Fig. 1. Plasmon oscillations in metallic nano-sphere in the presence of electric field [15].

When electrons and nuclei are displaced relative to each other, restoring forces originate from Coulomb's attraction. This results in oscillations in the electron cloud. The oscillation frequency is determined by four factors: density of electrons, effective mass of electrons, shape, and size of the charge distribution. Because it is a collective oscillation of electrons, it is called dipole plasmon resonance. In metals like gold and silver, plasmon frequency is influenced by electrons in other orbitals, such as the d-orbitals, which makes calculating plasmon frequency problematic using electronic structure calculations. Plasmon frequency, however, is easily related to metal dielectric constants (or refractive indices), which are observable as a function of wavelength for bulk metal. The correlation between the dipole plasmon frequency of a metal nanoparticle and its dielectric constant is done by considering the interaction between light and a spherical particle whose wavelength is much larger than size of particle. In these conditions, the electric field of light can be treated as constant, with interactions being described by electrostatics rather than electrodynamics. The localized surfaces plasmon resonances (LSPRs) occur when visible light causes electrons inside metals to oscillate collectively. A LSPR system oscillates as a combination of an electron density and an electromagnetic wave. This is different than surface plasmons, which are electromagnetic waves propagating along a metal-dielectric interface. In contrast to surface plasmon-polaritons, LSPRs may not require phase matching for direct excitation by incident light. A curved surface of the nanoparticle exerts a powerful effect on driven electrons, as a result of which a resonance occurs and the field amplification happen both inside and outside the nanoparticle. As a result, nanoparticles of metal scatter light at the LSPR frequency effectively. In metal nanoparticles, LSPR is the most efficient way for light to interact with matter and it determines the optoelectronic properties of the particles. A wide spectrum of LSPR frequencies can be tuned by fitting nanoparticles of different shapes and sizes to the surrounding medium or by altering the refractive index of the medium. The resonance in gold and silver nanoparticles occurs in the visible region of the electromagnetic spectrum. It is evident from the bright colors flashed by these particles submerged in transparent matrix (such as glass or aqueous suspension) in both transmitted and reflected light [15].

3. Methodology

The blue shift of semiconductor nanoparticles is caused by electron/hole quantization and produced significant changes in their optical properties. The dielectric phenomenon is used to explain the changes of metallic nanoparticles. The Laplace and Maxwell equations are solved to see how electric fields interact with a spherical nanoparticle under the two boundary conditions: 1) Surface of the sphere has a continuous electric potential, 2) Electric field displacement has a continuous value. The nano-sphere absorbs a portion of the radiation, scatters a portion of it, and may transmit a portion. The absorbing, scattering, and extinction peak spectra are made by solving these equations. The extinction coefficient, composed of the sum of the absorption and scattering coefficients, represents the total amount of radiation that is intercepted by each nanoparticle. In order to simulate the behavior of metallic nanoparticles in contact with light, the Nanosphere Optics Lab Field Simulator can be used [11]. In this simulator, Mie's theory is used to calculate metallic spherical nanoparticles' absorption, scattering, and extinction spectra. We used this tool to calculate the electric field distributions caused by electromagnetic radiation, as well as the absorption, scattering, and extinction of radiations by Au-nanospheres. In order to obtain results and predict the nature of nanoparticles, various factors including the refractive index of the surrounding medium, the radius of the nanoparticle, and the polarization of the incoming light can be varied. As a first step, we calculate the wavelength at which the extinction spectrum reaches its maximum for a nanoparticle of a given size, with the electric field held constant. The maximum electric field is found at the wavelength of the extinction peak, so this wavelength is assigned to the incident light and 'Calculate Electric Field' is clicked. We then calculate the various extinction spectra and the electric field distributions for Au nanoparticles based on incident radiation at wavelengths of 573nm.

4. Results & discussion

The electric field enhancements $|E|$ for 10, 20, and 30nm Au nanospheres are shown in Fig. 2 for light with wavelength equal to 573nm wavelength incident on them. The plots are drawn on two planes: one formed by the polarization and \mathbf{k} vectors (Fig. 2. a, b, c),

and the other perpendicular to the polarization vector (Fig. 2. d, e, f). The electric field in the vicinity of 10nm particles appears less distributed, but the intensity of the field is higher. The electric field intensity for 30nm particles is distributed across space, its intensity is lower than for 10nm particles. So, this result indicates an increase in electric field distribution with increasing nanoparticle size, but a decrease in intensity. A nanosphere within a dipole field exhibits smooth electric field distributions with symmetrical d-orbital lobes, as displayed in the Fig. 2. The absorption, scattering, and extinction (absorption plus scattering) spectra of gold nanoparticles of sizes 10, 20, and 30nm when light with a wavelength of 573nm is incident on them is shown in Fig. 3. Absorption and scattering efficiencies peak at different wavelengths and in different magnitudes. Light scattering is minimal for 10nm nanoparticles and maximum for 30nm nanoparticles, indicating strong size dependence. The three peaks observed in extinction spectrum, between 200-900nm wavelength-range, as tabulated in table 1. As the particle size increases, the wavelength at which the extinction coefficient peak occurs also increases. The most prominent peak is found at the least wavelength value.

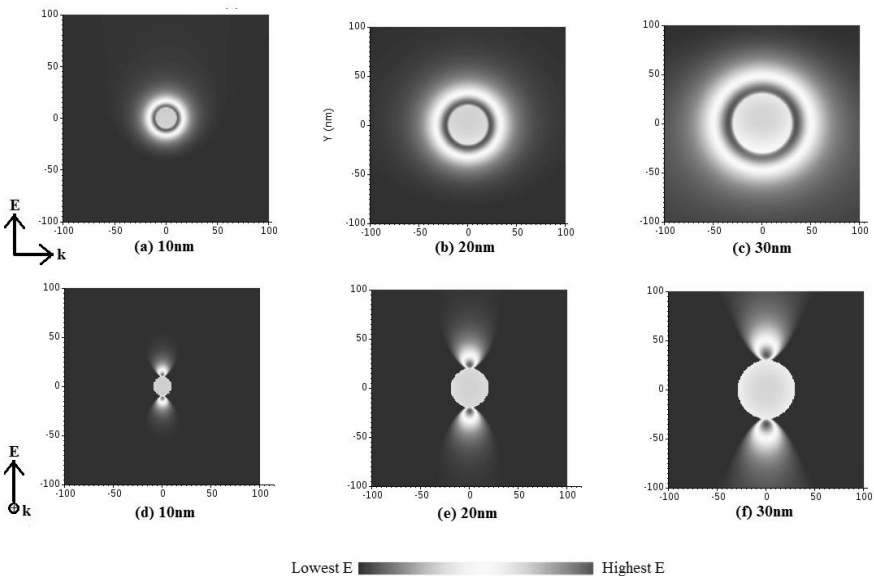


Fig. 2. Electric field distributions for radius 10, 20, and 30nm Au-Nano spheres. (Fig. a, b, c) for cross-section containing the propagation vector and polarization axes and (Fig. d, e, f) for cross-section perpendicular to propagation.

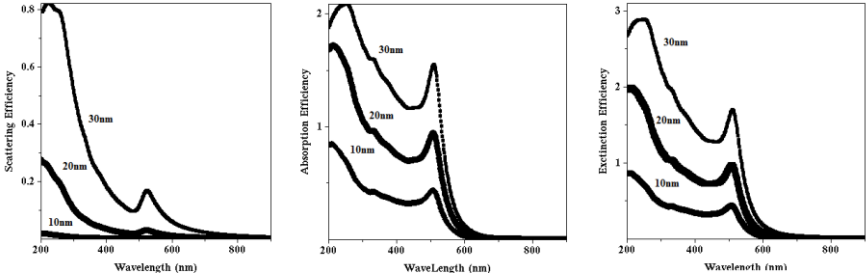


Fig. 3. (a) Absorption, (b) scattering, and (c) extinction efficiencies for Au-Nano spheres of size 10, 20, and 30nm.

Table 1. Peak extinction coefficients parameters for small size Au-Nano spheres of size 10, 20, and 30nm.

| Size of Au-Nano particle (nm) | Wavelength for Extinction coefficient peaks (nm) | Peak strength for Extinction coefficient peak |
|-------------------------------|--|---|
| 10 | 211, 331, 507 | 0.86 at 211nm |
| 20 | 212, 329, 508 | 1.98 at 212nm |
| 30 | 236, 250, 511 | 2.88 at 236nm |

In Fig. 4, results show how electric fields vary for bigger Au nanospheres with lengths of 25, 50, and 75nm. Further, increases in nanoparticle size lead to an even more diffuse electric field with a lower intensity as the field becomes larger. In the vicinity of a nanosphere, the electric field contours become more asymmetrical. The electric field variations of metallic nano-particles confirm the hybridization of plasmon modes near-field enhancements as demonstrated by Huang *et al.* [16]. However, metallic nanoparticle plasmonic resonances are still under intense investigation in order to help develop practical nanoscale optical sensors [17].

Fig. 5 shows the extinction spectra of big Au nanoparticles in two ranges (a) 25-75nm and (b) 100-200nm. As the size of Au nanoparticles increases, the peak extinction wavelengths increase in 25-75nm range, so there is a redshift in the peak extinction wavelengths. On the contrary, in 100-200nm range opposite is observed *i.e.* the peak extinction wavelength decreases, exhibiting a blue-shift. When the nanosphere size increases, the peak extinction amplitude changes less dominantly, and the bandwidth also decreases remarkably in the range 25-75nm than 100-200nm. This may be attributed to increased polarizability of larger particles. In

addition, the electric field distribution around the particle confirms the effect of particle size on optical transitions. As the nanoparticle size increased further, more than 100nm, there is a decrease in extinction efficiency. It may be due to the fact that for larger particles scattering dominates the absorption. In fact, a curve flattening is observed beyond 250nm that illustrate the four regime behavior for extinction spectrum. Fig. 3 (c) and Fig. 5 illustrate how nanoparticles of larger size are clustered together and have wider peaks than nanoparticles of smaller size. As a result, we may draw inference that Au-nanoparticles have different properties based on their size range. The four regime demarcations may be drawn at radii 25, 75 and 250nm for gold nano-particle.

The surrounding medium also plays an important role in determining the optical transitions caused by nanoparticles. The effect of water media on Au nanoparticles of size 25nm on extinction efficiency is shown in Fig. 6. There is a strong dependency between the magnitude of the peak as well as its position depending on the media type. Due to this dependence, water-immersed Au-nanoparticles may find a new application in the field of LASER generation [18] and third-order nonlinearity generation [19].

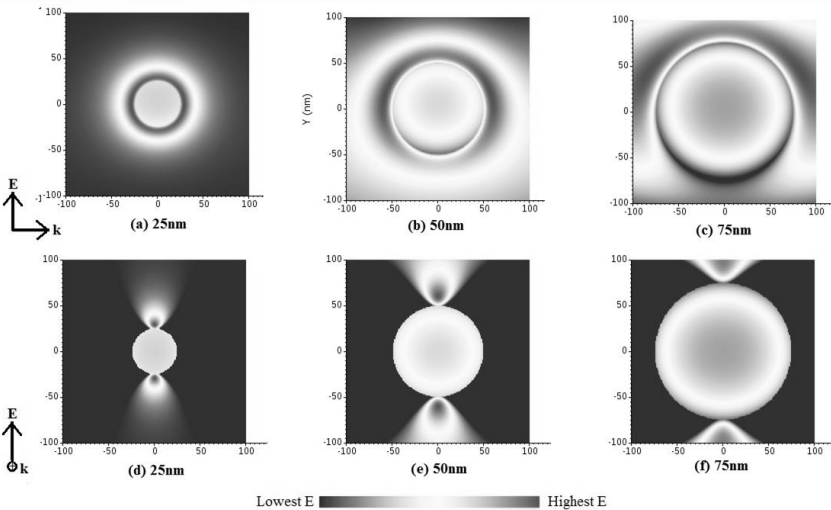


Fig. 4. E-field intensity variations for radius 25, 50, and 75nm Au-Nano spheres. (Fig. a, b, c) for cross-section containing the propagation vector and polarization axes and (Fig. d, e, f) for cross-section perpendicular to propagation.

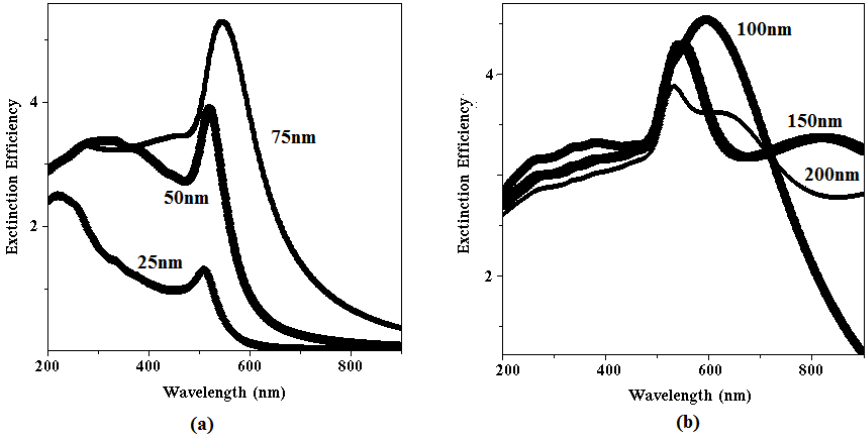


Fig. 5. Extinction efficiencies for Au-Nano spheres of sizes (a) 25, 50, and 75nm, and (b) 100, 150, and 200nm.

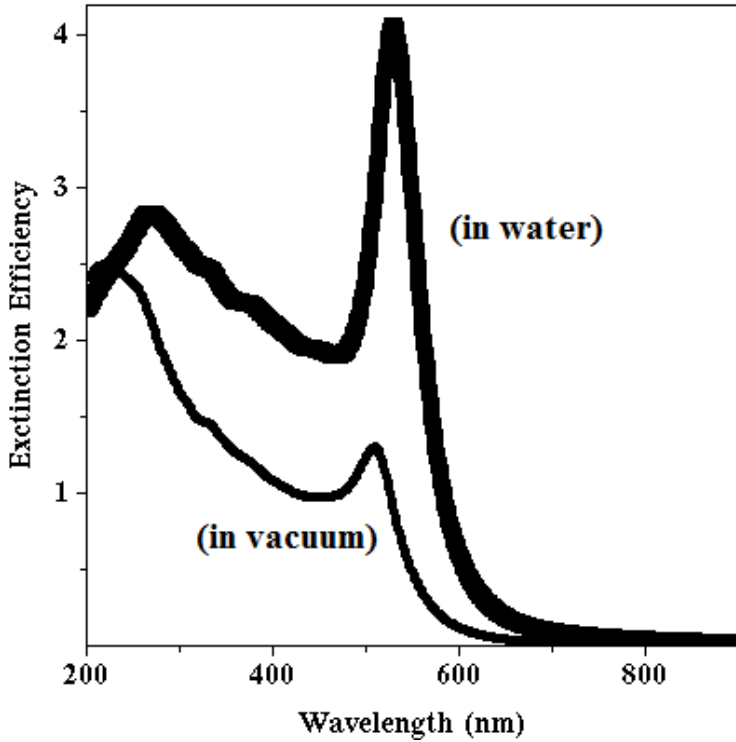


Fig. 6. Extinction efficiencies for Au-Nano spheres of size 25nm in vacuum and water media.

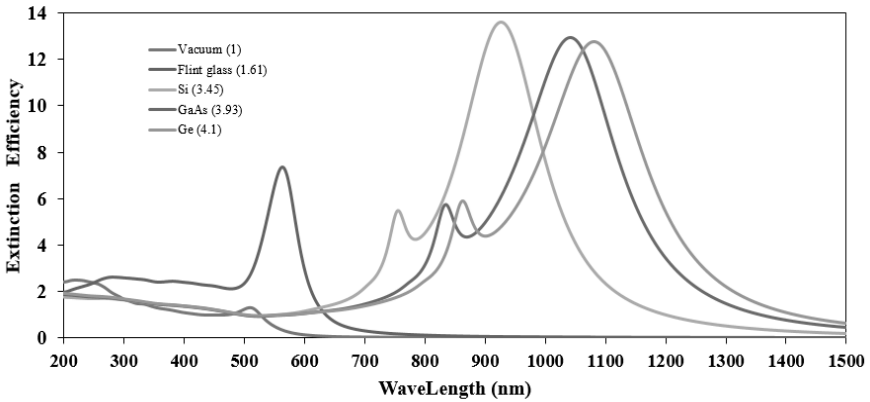


Fig. 7. Extinction spectra of 25nm gold nanoparticle when it is placed in different solid mediums with different refractive indexes.

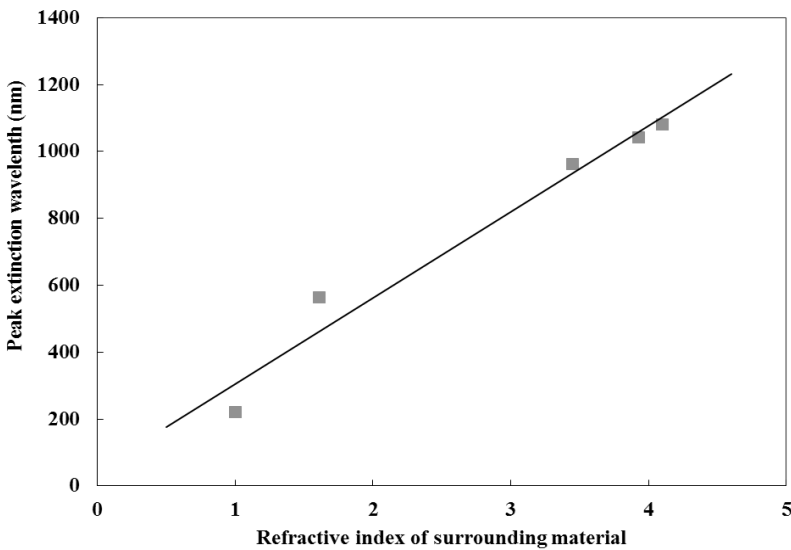


Fig. 8. Peak extinction wavelength variation for 25nm gold nanoparticle when it is placed in different solid mediums with different refractive indexes.

Fig. 7 shows how the extinction spectrum of a 25nm gold nanoparticle varies when placed in different solid mediums, such as Flint glass, Si, GaAs, and Ge, while vacuum indicates there is no

solid medium present. The wavelength, at which extinction peak occurs, varies with refractive index of the medium. The extinction peak is found maximum in the Si medium. When nanoparticles are embedded in solid semiconductor media, the field intensity is found to be greatly reduced, and the quantum of the decrease, increases with the refractive index of the solid. The peak extinction wavelengths are found to be red-shifted linearly as the refractive index of the surrounding medium increases as depicted in Fig. 8. Thus, linear dependence of extinction cross-section on refractive index of the medium is established.

5. Conclusions

An understanding of optical interactions with metallic nanoparticles is vital to explain numerous physical phenomena and helps in finding real-world applications. The present study examined how gold nanospheres' extinction spectra and electric field intensity varied with their sizes and surrounding medium. It is found that the electric field has a radially-distributed character that is governed by collective excitation of conduction electrons. The electrons in metallic Au-nanospheres, oscillate coherently when exposed to visible or near-IR frequencies of electromagnetic spectrum as evident from electric field distribution patterns. A near-field enhancement in plasmon modes is confirmed by the electric field variations of metallic nanoparticles. The scattering of light at 10nm nanoparticles is minimal, and at 30nm nanoparticles the scattering is maximal, indicating strong size dependence. A redshift in peak extinction wavelengths is observed when the nanoparticle size is increased for Au nanoparticles between 25-75nm. However, in the 100-200nm range the opposite is observed, *i.e.*, the peak extinction wavelength decreases, showing a blue-shift. As the nanosphere size increases, the peak extinction amplitude changes less pronouncedly, and the bandwidth decreases much more rapidly in the range 25-75nm than 100-200nm that may be attributed to increased polarizability of larger particles. In the case of nanoparticles larger than 100nm there is a decrease in extinction efficiency because scattering from larger particles dominates the absorption. Thus, gold nano-particles have different properties based on their size range,

and the present study indicate four regimes that can be defined with approximate demarcation radii 25, 75, and 250nm. On Au nanoparticles of size 25nm, water media affect extinction efficiency by affecting the magnitude of the peak as well as its position. The optical interaction efficiency of gold nanoparticles is found to increase linearly with the increase in size (in regime 25-75nm) and refractive index of surrounding medium. According to the findings presented in this article, gold nanoparticles have strong potential for a variety of applications including sensors for medical health care, industrial catalysts, and consumer products, if these uses extinction coefficient to quantify the parameter. The efficiency for such application is found to be improved in the size regime 25-75nm radii and that could be further enhanced by embedding in solid with higher refractive index.

References

1. S. S. Salem, A. Fouda, *Biol Trace Elem Res* 199, 344–370 (2021).
<https://doi.org/10.1007/s12011-020-02138-3>
2. S. Sreelakshmi, P.K. Vineeth, A. Mohanan, and N.V. Ramesh, *Materials Today: Proceedings*, 46(8), 3079-3083, (2021).
<https://doi.org/10.1016/j.matpr.2021.02.585>
3. Z. Huaizhi, N. Yuantao, *Gold Bull* 34, 24–29 (2001).
<https://doi.org/10.1007/BF03214805>
4. D. Pal, C. K. Sahu, A. Haldar, *J. Adv. Pharma. Tech. & Res.* 5(1), 4 (2014). <https://doi.org/10.4103/2231-4040.%20126980>
5. T. Patil-Bhole, A. Wele, R. Gudi, K. Thakur, S. Nadkarni, R. Panmand, B. Kale, *J. Ayur. Inte. Medi.*, 12(4), 640–648 (2021).
<https://doi.org/10.1016/j.jaim.2021.06.017>
6. W. Paul, C. P. Sharma. *Int J Ayur. Res.* 2(1):14-22 (2011).
<https://doi.org/10.4103/0974-7788.83183>
7. K. Khoshnevisan, M. Daneshpour, M. Barkhi, M. Gholami, H. Samadian and H. Maleki, *J. Drug Targeting*, 26(7), 525-532 (2018).
<https://doi.org/10.1080/1061186X.2017.1387790>

8. D. Aleksa, et al. ACS Nano 14(12) 17597-17605 (2020). <https://doi.org/10.1021/acsnano.0c08431>
9. K. V. Pereira, R. Giacomeli, M. G. de Gomes, S. E. Haas, Placenta, 100, 75, (2020). <https://doi.org/10.1016/j.placenta.2020.08.005>
10. P. Slepicka, N. S. Kasálková, J. Siegel, Z. Kolská and V. Švorcík, Materials, 13(1), 1, (2020). <https://doi.org/10.3390/ma13010001>
11. B. Tejerina, T. Takeshita, L. Ausman and G. C. Schatz, "Nanosphere Optics Lab Field Simulator," Nano hub, 2014. <https://doi.org/10.4231/D3FF3M064>
12. E. G. Wigglesworth, J. H. Johnston. Nanoscale Advances, 3(12), 3530-3536 (2021). <https://doi.org/10.1039/D1NA00148E>
13. A. F. Najafabadi, B. Auguie. Materials Advances, 3 (2022). <https://doi.org/10.1039/D1MA00869B>
14. A. Kumar, J. Adv. Sci. Res., 12 (ICITNAS), 223-229 (2021).
15. K. L. Kelly, E. Coronado, L. L. Zhao and G. C. Schatz, J. Phys. Chem. B, 107, 668, (2003). <https://doi.org/10.1021/jp026731y>
15. Y. Huang, L. Ma, M. Hou, J. Li, Z. Xie and Z. Zhang, Scientific Reports, 6, 30011 (2016). <https://doi.org/10.1038/srep30011>
16. S. Kaushal, S. S. Nanda, S. Samal, and D. Kee Yi, ChemBioChem, 21(5), 576, (2020). <https://doi.org/10.1002/cbic.201900566>
17. H. Huang and Leonid V. Zhigilei, J. Phy. Chem. C, 125(24), 13413, (2021). <https://doi.org/10.1021/acs.jpcc.1c03146>
18. S. Altowyan, A. M. Mostafa and H. A. Ahmed, Optik, 241, 167217 (2021). <https://doi.org/10.1016/j.ijleo.2021.167217>